Pergamon

Cement and Concrete Research 30 (2000) 101–116

CEMENT AND CONCRETE RESEARCH

A model for the microstructure of calcium silicate hydrate in cement paste

Hamlin M. Jennings*

Departments of Civil Engineering and Materials Science and Engineering, Northwestern University, Evanston, IL 60208, USA

Received 18 May 1999; accepted 27 September 1999

Abstract

A model is proposed for the structure of calcium silicate hydrate (C-S-H) as it is formed during the hydration of Portland cement. One purpose of the model is to move toward an ability to evaluate the microstructure quantitatively, so that it can be related to properties on the one hand and processing on the other hand. It is a hypothesis intended to promote discussion and motivate experiments. Furthermore, the model is an attempt to rationalize disparate measurements of specific surface area reported in the literature by describing an underlying structure, which, when observed by different instruments, gives different results. It is a simplified representation of the microstructure within the size range of about 1 to 100 nm. The basic building block is a unit of C-S-H that is roughly spherical and approximately 2 nm across with a specific surface area of about 1,000 m^2/g. These building blocks flocculate to form larger units. This paper describes the structure of the basic units and how they pack to form larger structures and microstructures. The model also explains a number of variant observations for such measured attributes as specific surface area, pore size, and density as determined by different techniques, as well as water content at different relative humidities.

Keywords: Calcium-silicate-hydrate (C-S-H); Crystal size; Microstructure; Pore size distribution; Surface area

1. Introduction

A great deal of information about the structure of calcium-silicate-hydrate (C-S-H) at the atomic scale has been obtained and refined during the last decade [see for example 1–5]. It can be visualized as tobermorite with many imperfections and irregularities such that it becomes nearly amorphous, possibly intermixed at a very fine scale with a similar version of jennite. This is consistent with a variety of experimental results, and although details remain a topic of discussion, the structure on the atomic scale is fairly well understood.

Between about 1 and 100 nm, however, the structure or microstructure of C-S-H has not been modeled precisely. The problem is that direct investigation using techniques such as microscopy has only provided fragments of information that are mostly qualitative. Attempts to evaluate the microstructure by surface area and pore size distribution, approaches that provide great insight for other materials, have proven particularly frustrating for C-S-H. Not only do different techniques provide different values, but also some techniques, such as nitrogen adsorption, give inconsistent results on apparently similar samples.

Physical properties such as changes in mass, strength, modulus, and dimensions due to drying at specific relative humidities (rh) have been used to deduce structure at about the 1- to 10-nm scale, and several models are in the literature [6–8]. The most detailed and widely used model is that of Feldman and Sereda [6], which was slightly modified by Daimon et al. [9]. The Feldman-Sereda model represents a triumph in deducing specific characteristics of the microstructure by finding a "hidden" structure that is consistent with a variety of observations, even though the structure cannot be observed directly. There are, however, some nagging questions. How does the model structure relate to physical characteristics such as specific surface area (SSA), and why is the value of SSA so strongly dependent on the technique used? Why is there no way of quantitatively characterizing the structure? Is the structure homogeneous at a scale greater than 1 to 10 nm, and if it is not, can the heterogeneous distribution of material be characterized? How can the structure be related to properties?

The picture has not been made any clearer with the availability of new techniques that provide measures of SSA and pore size, such as small angle neutron scattering (SANS), small angle X-ray scattering (SAXS), and nuclear magnetic resonance (NMR). Values of SSA range from about 25 to 700 m^2/g for highly hydrated paste, a confusingly large range that, without supposing massive weaknesses in the analysis, suggests that some of the techniques are invalid because they include in-

* Corresponding author. Tel.: 847-491-4858; fax: 847-491-3109.
E-mail address: h-jennings@nwu.edu

0008-8846/00/$ – see front matter
PII: S0008-8846(99)00209-4

ternal or interlayer surfaces that are not part of the pore system, and/or they miss some of the surface area. These results, reviewed recently by Thomas et al. [10], only broaden the debate about the "true" SSA and the implied microstructure.

This paper describes a model for the microstructure of C-S-H at the scale between 1 and 100 nm. The model is for an underlying structure that is not directly observable, and it represents an attempt to reconcile several apparently disparate observations. It is a model that can be used to explain surface area, pore size distribution at the fine scale, and the density and the water content at various rh's. Other characteristics such as fractal dimension are also considered. It is hoped that the hypothesis will serve as a basis for discussion and a motivation for experiments.

2. Background summary of observations

Because this paper is concerned with the microstructure of C-S-H and not with other phases usually present in cement paste, the units of SSA are normalized per gram of D-dried C-S-H (ground C-S-H equilibrated to a water vapor pressure of 0.5 μm of Hg) as opposed to (for example) per gram of paste, and will hereafter be referred to as specific surface area or SSA. As pointed out by Thomas et al. [10], there are problems connected with the translation of the raw data into SSA, particularly if normalized to the quantity of C-S-H. It is tempting to suggest that one or more of the reported values are suspect, but this would not explain the very large variation in the values reported. Here, the assumption is that all values provide important information. However, even though every effort has been made to compute accurate values as normalized per gram of D-dried C-S-H, the inherent errors and assumptions, such as degree of reaction for reported SSA (which are not always reported in the appropriate papers and are therefore only estimated), mean that the model proposed here can only provide predictions for large trends and cannot be used to generate precise numbers. However, if the model has value, then further research can make it more precise. Much of the uncertainty would be removed if SSA were reported per gram of ignited C-S-H. This is difficult for historical data but may be considered in the future.

Recent analyses [11,12] show that exact mathematical expressions for rates of reaction between cement and water are achieved by dividing the reaction into three stages. This approach is consistent with other studies [13,14] that showed that certain features in the microstructure form at certain times; as a result the reaction was divided into early, middle, and late periods. The first stage is a period of possibly diffusion-controlled slow reaction, called the "early period," that ends at the time of initial set. Second, there is a nucleation and growth stage lasting until 12 to 14 h, or possibly the first day, called the "middle period." Finally, there is the "late period," or diffusion-controlled stage, for the remaining duration of the reaction. This model considers only the development of C-S-H in the last two stages, namely the middle period and the late period. Only a small amount of product with a unique structure forms during the early stage, and it is not considered here.

Most of the data in the literature are for pastes with a water/cement ratio close to 0.4, which serves here as the starting point. Typical degree of reaction vs. time information is included in Fig. 1. Some of the key data in the literature for SSA obtained by different techniques for the middle and late periods are included in Tables 1 and 2 [15–30]. Finally, some information about composition and moisture contents at different relative humidities is included in Table 3 [31–35].

An important observation for the model reported here is that the SSA as measured by nitrogen has been modeled successfully [27,36 (referred to here as the J-T model)] with the assumption that there are two types of C-S-H, one into which nitrogen can penetrate and one into which nitrogen cannot penetrate. The J-T model does not incorporate the intuitive assumption that a higher SSA is simply associated with C-S-H that has a more open structure, and that otherwise C-S-H has a constant density. Careful measurements and analyses show that the higher SSAs related to variables such as higher initial water/cement ratio are also associated with a larger volume of fine gel pores that are not assessible to nitrogen (meaning that the density measured by nitrogen is not constant), a counterintuitive result. It should be noted, however, that this is not the case when SSA is influenced by drying technique. In this case higher SSAs are associated with a more open structure and therefore greater volume of gel pores.

Recently a physical basis for the J-T model has been developed [27], namely, that the two types of C-S-H have different densities as seen by nitrogen: a high density C-S-H (HD C-S-H) and a low density C-S-H (LD C-S-H). Independent observations of the development of surface area from neutron scattering compared to degree of hydration, as shown in Fig. 1 [18], suggest strongly that two types of C-S-H are present in cement paste. The explanation for Fig. 1 is that the surface area of one of the types is not seen by neutrons, and therefore when it forms, surface area and percent reacted do not scale linearly. After the model is optimized, the two densities, based on the model for nitrogen surface area alone for dry C-S-H, are HD = 1,670 kg/m^3 and LD = 1,400 kg/m^3. These are relatively low densities and cannot be explained by atomic arrangement because they are much lower than that of C-S-H, excluding any gel pores (somewhere around 2,500 kg/m^3), and therefore they must contain some gel porosity. If the pores within these structures are filled with water, the density becomes a more typical 1,900 kg/m^3, as will be discussed below. In the model described here, HD C-S-H is made up of densely packed particles into which nitrogen cannot penetrate. Particles of LD C-S-H are not packed as tightly, and nitrogen can penetrate partially into this structure and around the LD particles to give a surface area, which according to the J-T model is about 220 m^2/g of LD C-S-H. For the J-T model of nitrogen surface area,

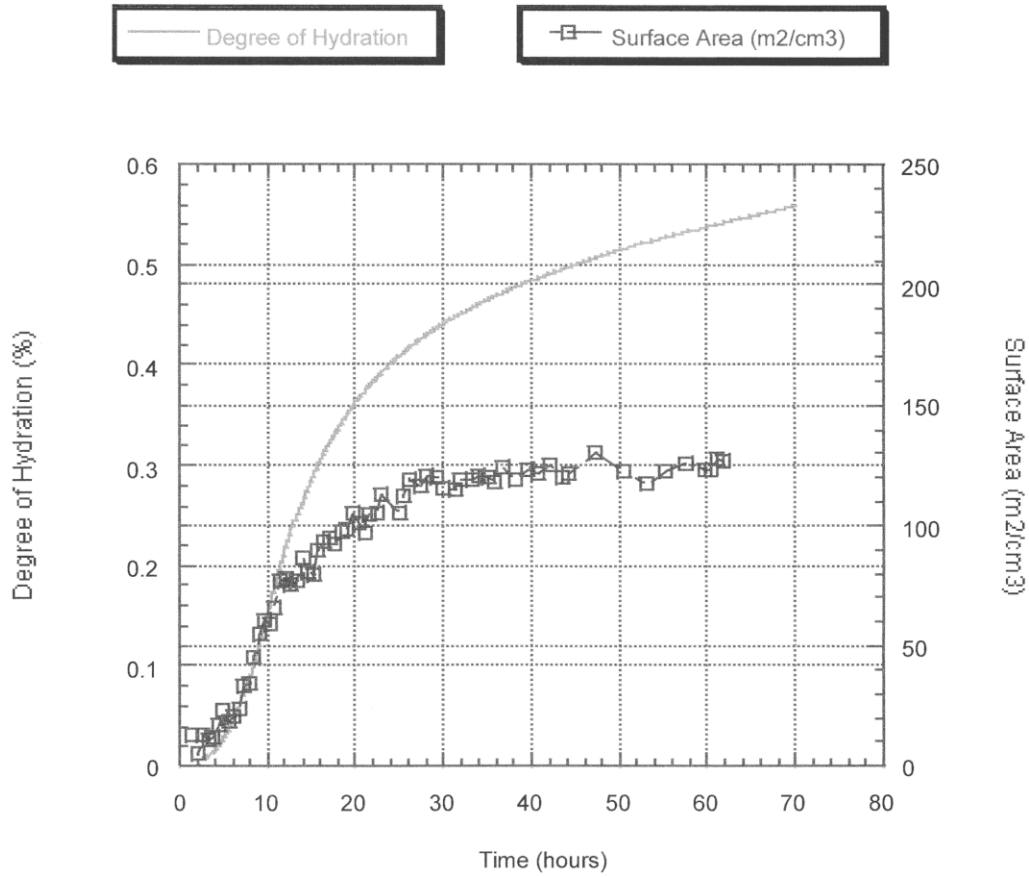

Fig. 1. Degree of reaction and rate of reaction for a typical cement paste with water/cement ratio of 0.4. after Thomas et al. [18]. Note that the surface area is in units of m^2/volume as per original analysis, and degree of reaction is derived from original heat evolution data. The observation that after about 12 to 14 h the surface area does not continue to rise at the same rate as the amount of reaction product suggests indicates that the product formed during the late stage has only a small surface area on average.

higher measured SSAs simply mean that there is a greater proportion of LD C-S-H.

One problem with interpreting SSA measurements is the definition of the surface. A great deal of attention has been paid to how a technique might mistake interlayer space for surface, or how very small "ink bottle" entrances might prevent a gas from "seeing" some surfaces. The model described here does not lead to a unique SSA, but rather defines SSA as a value that depends on the scale or resolution of the probe. As described later C-S-H is one of nature's true fractals within the size range of this model. Therefore, it is inaccurate to describe the structure as being made up of specific building blocks of specific size and density since the size of the building blocks must be somewhat blurred over different scales, which was also the essence of the Feldman-Sereda model [6]. However, to construct the model, certain specific sizes must be considered. The scales chosen are dependent on the experimental technique used to obtain the data. Therefore, in this microstructure model, a smaller probe "sees" a greater surface area. Some techniques "see" only the LD C-S-H with its coarser porosity, and some see both LD and HD C-S-H. The J-T model can specify the relative amounts of LD and HD C-S-H.

Table 1
Specific surface area (m^2/g C-S-H), middle period

Technique	12 hours	24 hours	Condition of sample or assumption	References[a]
SAXS	620	800	Wet cement paste	[15]
NMR	700	1,000	Assume 35% reacted at 24 h; sealed cement paste	[16,17][b]
SANS	390	280	Wet if $\rho = 2{,}180$ kg/m^3; sealed C_3S paste	[18]
Sorption N_2		200	Careful dry, C_3S paste	[19]
		100	D-dried	[20]
		55	Oven dry	[20]
Sorption H_2O	500	450		[21]

[a] Source of primary data.

[b] Reference 16 contains corrected information that was originally published in reference 17.

3. The microstructure model

The model is the result of an iterative process of proposing a combination of structures at different scales and then

Table 2
Specific surface area (m^2/g C-S-H), "mature" late period

Technique	SSA if all C-S-H included	SSA if only LD C-S-H 0.5 of total	Condition of sample, wavelengths of radiation, r = size of feature	References
SAXS	1,000	–	Wet, $\lambda = 0.071$ nm	[15,22]
	425		11% rh (approximately)	[22]
	320		D-dry	[22]
	195		Oven dried	[22]
SAXS	350		$\lambda = 0.154$ nm	[23,24]
NMR	1,000 at 3 days (assume 46% reacted)		pore size $r = 2.5$ nm	[16,17]
	700 at 28 days (assume 70% reacted[a])		pore size $r = 11$ nm	
SANS	230	460	$\lambda = 0.5$–0.8 nm, $\rho = 2180$ kg/m^3; characteristic length, 2.5 nm[b]	[25,26]
Sorption N_2		230	Model for dry	[27]
	230	460	Very careful dry	[28,29]
	110	220	Solvent exchange	[20,28]
	55	130	Oven dry	[20]
Sorption isopropanol	60	120		[30]
Sorption H_2O	320			[21]

[a] Sample was sealed, and it may have self-desiccated somewhat.
[b] Size of particle or pore.

testing it against the observations. The main criterion for accepting any proposed structure, one that cannot be "seen" directly, is that it is self-consistent with as much of the experimental data as possible. The boundary conditions placed on the model are SSAs, densities, pore sizes, and water content at different moisture conditions. When results vary from one technique to another, the interpretation is that they resolve different scales in the structure. Furthermore, any model for the structure of C-S-H within the size range of 1 to 100 nm must mesh with what is known about the structure at finer and coarser levels. Finally, the observation that complete hydration is only possible at water/cement ratio >0.4 should be accounted for. Experimental values from the literature are displayed in Tables 1, 2, and 3. It becomes a challenge to try to understand the relationship between values measured for samples that were saturated and values measured for samples that were dried. This will be discussed later.

If we assume the basic building blocks are spheres, then density and specific surface area are related by Eq. (1):

$$S = \frac{3}{\rho \cdot r} \tag{1}$$

Table 3
Measured and computed density for C-S-H at three rh conditions

Condition	Composition	Measured density (kg/m^3)	Comment and reference	Calculated density[a] from composition (kg/m^3)	Assumption for density and molar volume[d] of basic unit	Pore volume to accommodate added water based on composition (percent)	Model pore volume based on density and surface area (percent)
D-dry	1.7 CaO • SiO_2 • [1.3–1.5] H_2O, GMW = 178	2,440–2,500[b]	He Methanol [31,32]	–	mv = 63.6		
		2,700–2,860[c]	H_2O [33,34]	–	mv = 72.7		
0.7 H_2O added 11% rh	1.7 CaO • SiO_2 • 2.1 H_2O	2,180	Computed [35]	2,240	ρ D-dry = 2,450	17[e]	18
		2,430–2,450	He [31]	2,500	ρ D-dry = 2,800	15[e]	18
2.6 H_2O added Saturated	1.7 CaO • SiO_2 • 4 H_2O	1,850–1,900	Computed [35]	1,880	ρ D-dry = 2,450	42[e]	35[f]
		1,900–2,100	Computed [32]	2,037	ρ D-dry = 2,800	39[e]	43[f]

[a] Calculation assumes mass and volume of water being added to pores is 1,000 kg/m^3.
[b] Range of measurements in the literature that are lower density.
[c] Range of measurements in the literature that are higher density.
[d] Molar volume = GMW/ρ with ρ in g/m^3 ($\times 10^{-6}$ m^3).
[e] Computed from molar volume of dry C-S-H and molar volume of water.
[f] Based on average density of 1,595 kg/m^3 with pores empty and appropriate density of basic unit (see text).

where S = surface area per gram of D-dried C-S-H (SSA), ρ = density of D-dried C-S-H, and r = radius. It must be stated clearly here that the building blocks are not spheres but rather roughly equiaxed units. However, spheres are easy to describe and useful for calculation. This point will be considered later in the paper.

Even a quick look at the data in Tables 1 and 2 suggests that the values for SSA during the middle stages are apparently quite different from the values obtained for mature specimens. Except for values measured by X-rays, SSA does not develop with a linear relationship to the amount of C-S-H. This phenomenon has been discussed by Thomas et al. [18] and used as support for the two types of C-S-H with the further observation that LD C-S-H forms during the middle period.

Obviously the values shown in Table 1 depend critically on determinations of degree of reaction. Values for SAXS and SANS used both calorimetry and loss on ignition, and as such, even if the exact values are challenged, the trends are probably accurate. Values for degree of reaction from NMR experiments are simply an estimate. Values for surface area using nitrogen are, at best, difficult to obtain during the middle period. The numbers, therefore, are presented only as evidence that this period is a period of dynamic change in the structure of C-S-H.

As shown in Table 3, the measured densities for each rh condition are divided into two ranges, which are not (at the moment) linked with the amounts of LD and HD C-S-H. They are simply experimental values. In other words, studies of densities reported in the literature for the three rhs included in Table 3 may be divided into two families: (1) higher density values and (2) lower density values, unrelated to HD and LD C-S-H. During the development of this model, it was realized that both the higher values and the lower values are self-consistent with the proposed model, but the higher and lower values could not be intermixed. The reason for these two families is unclear, as discussed later, but to fit the model, only one or the other can be used at a time. Both possibilities are developed here. Some evidence [25] suggests that the lower density is preferred, but recent results by the same authors indicate that perhaps the higher density is preferred. This model explores both possibilities.

3.1. Nucleation and growth, early age (middle period)

The middle period (4 to 24 h) is dynamic, and the structure of C-S-H changes rapidly with time. In this model, the middle period is one in which the smallest units are flocculating to form the microstructure, which is mostly LD C-S-H.

The density of the smallest unit that can be used to build the nanometer structure of C-S-H is taken as either 2,450 or 2,800 kg/m^3, which are typical of the values for densities reported in the literature. The former is the measured value using helium pycnometry, and the latter is a measured value using water to penetrate all possible porosity. The model does not depend strongly on the exact value chosen, but it is able to distinguish between the above values. If this smallest unit is associated with one of the higher surface areas in Table 1, say 800 m^2/g of C-S-H, then the unit, using Eq. (1), has a radius of either 1.5 or 1.4 nm depending on the density of the smallest unit, referred to here as the basic unit. In either case, although the unit may not be spherical (indeed it is probably not spherical), the dimensions are so small that they are near that of the repeat unit of a simple layer of tobermorite ($\sim 0.56 \times 78 \times 1.4$ nm), and therefore the basic unit must be roughly equiaxed, although almost certainly they are not symmetric. As will be discussed briefly later, these units are extremely small, and the influence of surface interactions with a gas or liquid may be great. Polar water may pack very efficiently at the surfaces, giving apparently high values for density. For any computed value using the density of the basic unit, the value based on the lower density is given first, and the value based on the higher density is included in parentheses.

During the first 14 h, the SSAs measured by SANS become smaller with time, as shown in Fig. 2 (J.J. Thomas, personal communication). This is taken to mean that the units are flocculating, and SANS sees the particles growing and not the internal structure. They probably have asymmetric surface change and therefore do not line up to form a long-range crystalline order. At the least, the system is dynamic at 12 h.

According to the model, the basic units pack together into an irregular three-dimensional structure, with an 82% packing factor. This gives a density of either 2,010 kg/m^3 (or 2,300) if dry, and 2,180 kg/m^3 (or 2,440) if the pores are filled with water. Both of these latter densities have been measured by different researchers for C-S-H at 11% rh, suggesting that in either case, under this condition these smallest pores are full of water. Eighteen percent pore is just enough to accommodate 0.6 moles of water at 1,000 kg/m^3 for each mole of C-S-H, and therefore, this porosity is also consistent with the composition reported in Table 3. The issue of 82% packing factor being too high for uniformly sized spheres will be discussed further in the section on fine-scale structure.

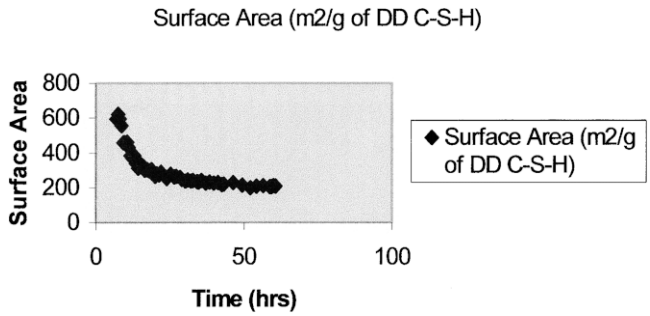

Fig. 2. Surface area per gram of C-S-H as measured by SANS vs. time. The surface area becomes smaller with increased degree of reaction for the first 24 h or so, and then remains nearly constant before slowly increasing with time (i.e., 28 days, not shown), courtesy of J. Thomas.

Just after the first day of reaction, when the flocculation process is nearly complete, the total SSA measured by SANS is 230 m^2/g. Since the structure is dynamic up to about 48 h, the density of the flocs is probably not constant during this period, but the most important point is that these measurements indicate some sort of aggregation or flocculation process is occurring. This model is based on the idea that the basic C-S-H units come together to form into two different structures: one from the flocculation of basic units that were dispersed in the larger capillary pore space, and one from basic units that form in much more confined space near the unreacted cement during the late stage. These are the LD and HD C-S-H structures. From this point onward, X-rays (and possibly NMR at least for the first several days before possible self-dessication) see all of the surface area, and SANS sees the SSA of 2.7 nm radius LD C-S-H units.

3.2. Late stage

During the late period, interpretation of the measured surface areas is complex if one is to rationalize all measured values including values from nitrogen sorption. The J-T model [27,36] for nitrogen surface area assumes that under normal conditions most, but maybe not all, of the LD C-S-H is formed during the middle period. This assessment may change with different water/cement ratios and other reaction conditions, especially after about 60% reaction. During the late stage, formation of HD C-S-H is predominant at water/cement ratio = 0.4. The HD C-S-H has a very fine internal structure, and therefore its surface area can only be measured by X-rays. This is not only the basis for explaining the values of the surface areas as measured by nitrogen, but it also accounts for the nonlinear relationship between degree of reaction and surface areas as measured by NMR, SANS, and nitrogen. Surface areas of mature samples vary widely as shown in Table 2. According to the J-T model, for a water/cement ratio of 0.4, 50% of the C-S-H is LD with a density as measured by nitrogen of 1,450 kg/m^3, and the rest is HD with a density of 1,750 kg/m^3 as measured by nitrogen. These densities cannot be measured directly but are determined (independently) from the J-T model based solely on nitrogen surface area and pore volume measurements for dry C-S-H. These densities are low and are really densities of assemblages of particles or globules. They are more fully described below.

3.3. Structure of the two kinds of C-S-H gel

Schematic representations of the two kinds of C-S-H gel are shown in Figs. 3 and 4. The small circles are the basic unit. Table 2 includes the surface areas that must be explained by the model, and Table 3 includes densities, measured and calculated based simply on composition. Table 4 shows results of densities of differently sized units under the two conditions in which its pores are empty or full of water. The idea behind the model is that everything becomes self-consistent. The fine-scale structure is described for the middle period, except the surface area is 1,000 m^2/kg. The basic spherical units cluster together (flocculate) to make globules (as described by Allen [26]) with a radius of 2.5 nm or less. The structure of the globules is deduced from SANS experiments [26] as coming from C-S-H with a composition equivalent to that measured for C-S-H in equilibrium with 11% rh, the condition for which a monolayer of water surrounds the globule. Furthermore, the globules in this model, for the higher density, have a radius of 2.8 nm, which are the only solid features near 2.5 nm. Since the pores within the globule are full of water down to 11% rh, it must be these features that are detected by SANS. In this model, therefore, water is contained within fine pores or interstitial spaces (solids being packed with 82% efficiency) at this rh. The surface area of the globule under this condition measured by SANS is 230 m^2/g of D-dried C-S-H. If SANS sees only globules in the LD C-S-H, the value for this portion of the C-S-H is 460 m^2/g. As a note to establish consistency, assuming X-rays see both structures, the 460 m^2/g value is bounded by the experimental values of 500 and 385 m^2/g for 52% rh and D-dried values, respectively (no measurements were made at 11% rh). In other words, SANS sees only the globules within LD C-S-H even under saturated conditions, and SAXS sees these globules only if dried to 11% rh, a condition under which the finer structure has collapsed. If the density of the globule is 2,180 kg/m^3 (2,440 kg/m^3), equivalent to 2,010 kg/m^3 (2,300 kg/m^3) when D-dried, but now including the empty, fine porosity, the globule has a radius of 3.2 nm (2.8 nm).

As shown in Figs. 3 and 4, representing an idealized 2-D structure, the globules pack together to form LD and HD structures that contain 28 and 13% porosity between the globules (i.e., excluding pores within the globules), respectively, (independent of the density of the basic unit used). The 28% porosity can be modeled by an imperfect closely packed structure (26% pore) and the 13% porosity by a squashed together closely packed structure. This will be discussed further later. If the surface area of LD C-S-H is measured by nitrogen, then the surface area of LD C-S-H as deduced by the J-T model is 250 m^2/g [27].

Another corroborating note is that the densities of 1,750 and 1,440 kg/m^3 average to 1,595 kg/m^3. This implies an average density of 1,942 kg/m^3 (or 2,170 kg/m^3) if the pores are filled with water. These numbers are based on nitrogen, and they agree with the measured saturated values as shown in Table 3. These numbers are also consistent with the volumes occupied by 2.6 moles of H_2O added to the basic unit to give a total of 4 moles of H_2O in a mole of saturated C-S-H. This is shown in the two columns on the right of Table 3 along with similar calculations for 11% rh.

These densities and volumes provide some insight as to how much reaction can occur in paste before the reaction stops for lack of volume. In the following reaction, the only unknown quantity is the molar volume of C-S-H [see Eq. (2)].

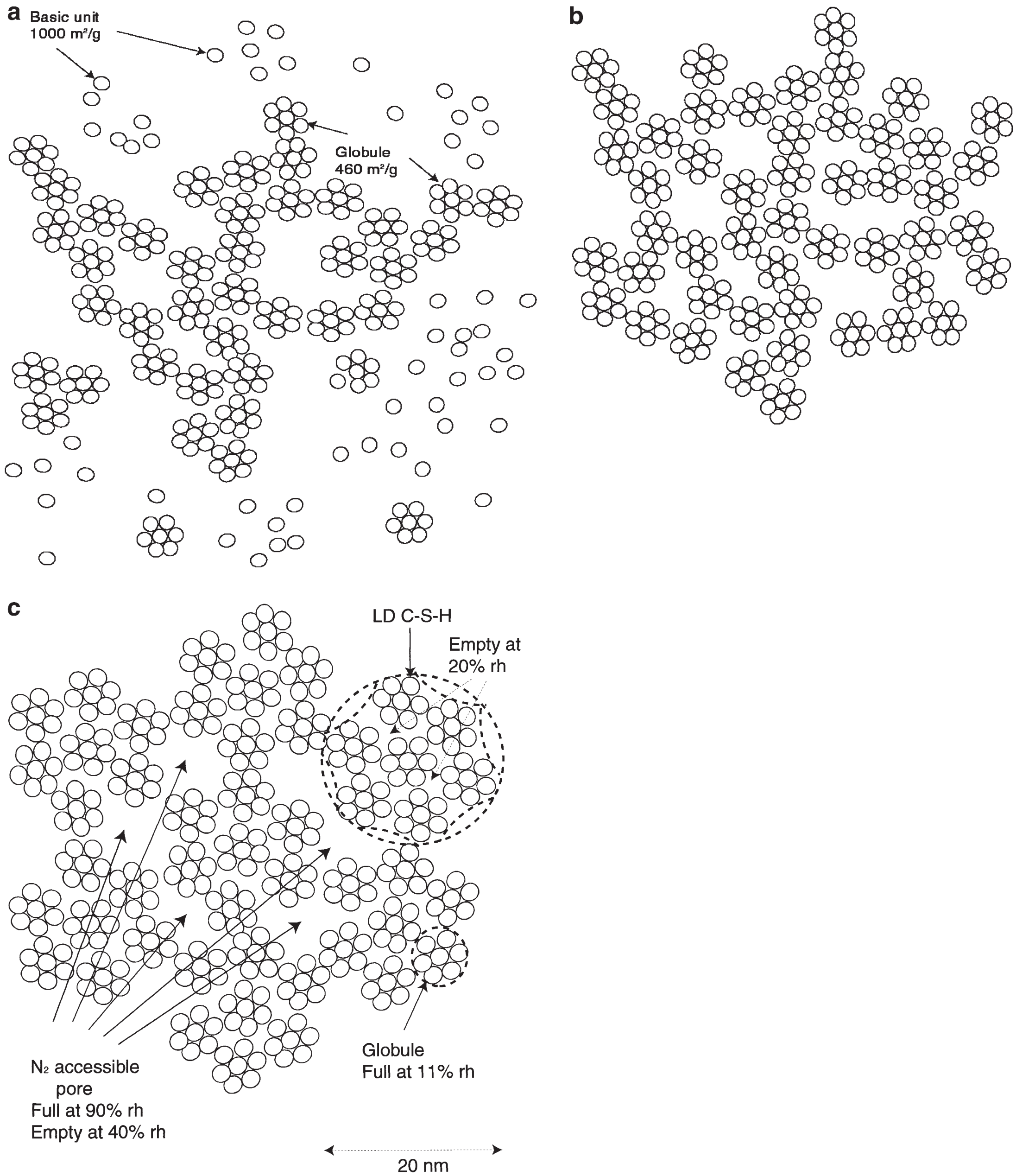

Fig. 3. (a) A 2-D schematic of semidispersed LD C-S-H formed during the first few hours in the middle period and in a saturated condition. (b) 2-D schematic of condensing LD C-S-H, possibly at about 6 to 10 h into the reaction. The smallest units may not be of constant size and are certainly not spheres. Also the globules may still be more dispersed. This representation is a working model. (c) 2-D schematic of LD C-S-H as formed by the late stage and/or by drying.

$$C_3S + 5.3H \rightarrow C_{1.7}SH_4 + 1.8CH \qquad \text{Chemistry}$$
$$(72.4^*) + 5.3(18^*) \rightarrow ? + 1.8(33.2^*) \qquad \text{Volume}$$
$$^*(10^{-6}m^3)$$
$$? = 125 \tag{2}$$

From the J-T model at water/cement ratio = 0.4, about half the C-S-H is LD and half is HD. This leads to an average wet density of 1,915 kg/m^3 (2,116 kg/m^3), which implies a molar volume (GMW/ρ) of 118 × 10^{-6}m^3 (107 × 10^{-6}m^3) (ρ = density in grams). This value provides just a little more volume than is necessary for complete hydration, which, in Portland cement with other phases reacting, is consistent with Powers' initial observations [32].

Similarly molar volumes for other water/C_3S ratios and other ratios of LD and HD in the product can be computed. At water/cement ratio of 0.25, the J-T model predicts 0.2 LD and 0.8 HD. Under this circumstance, if all of the water is conserved and only unreacted C_3S and reaction products are formed, reaction will stop at 65%. For water/cement ratio =

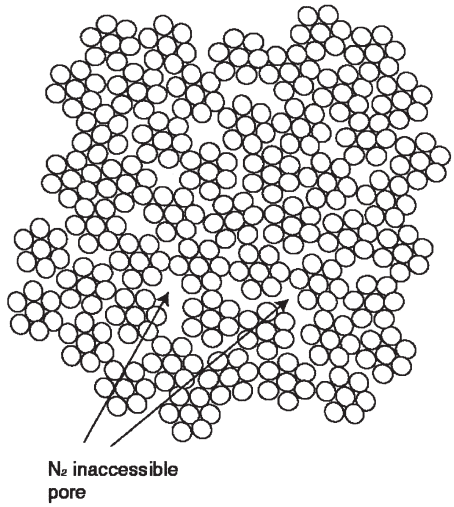

Fig. 4. 2-D schematic of HD C-S-H, the predominant type of C-S-H that forms during the late stage at water/cement ratio = 0.4

0.35, reaction will stop at 91%. These numbers are in good agreement with values for older pastes in the literature [19,30].

3.4. Pore size

The proposed model has some implications for measured pore size, although these implications can only be interpreted as trends. Nitrogen isotherms and NMR have been used to deduce pore size, and values are included in Table 5. The model constructs C-S-H from nested packing of variously sized units with specific size and packing efficiencies. As seen in Table 4, the size of pores in the model and those measured are in reasonable agreement, given all of the assumptions.

Daimon et al. [9] deduced that when calcium hydroxide was extracted from a paste, the pore size as measured by nitrogen became smaller even though the large CH crystals should have left large residual pores. They argued that this is because CH engulfed C-S-H, and therefore its removal exposed fine pores. In this model there are three possibilities: (1) that CH helps prevent the collapse of structure during drying, (2) that CH partially or wholly blocks some of the pores, or (3) both. Small, possibly amorphous, CH may well be found in the interstitial spaces as described in this model, and the removal could allow nitrogen to access the finest pores. Its removal could also allow the structure to collapse more easily during drying.

3.5. Fractal dimension

Of major importance in this model is the relationship between the structure and its SSA and its density, as seen at different scales. The finest scale is $r = 1$ nm with a density of 2,450 kg/m^3 (because log-log plots are to be considered, this value is not significantly different from 2,800 kg/m^3) and a surface area of 1,000 m^2/g. For this model, each scale "sees" a different surface area and density, which means that the structure may be fractal [26,37,38]. Log-log plots are shown in Fig. 5. In Fig. 5b an additional point has been placed at SSA = 120 m^2/g d-C-S-H, which is an area that may be measured by large molecules such as cyclohexane (data taken from Mikhail and Selim [30]). If the line is extrapolated, it provides a radius of 25 nm. This will be dis-

Table 4
Model values

Structure	Density (kg/m^3) computed from volume of solids and pores in the model		Radius nm, computed from density and surface area	Surface m^2/g
	Pores empty	Pores full		
Basic building block	2,450	2,450	1.2	1,000
	2,800	2,800	1.1	
Globules (individual)	2,010	2,180	3.2	460 SANS, S $(N)_2$, Table 2
	2,300	2,440	2.8	
LD	1,440	1,850[a]	9.3	250 from J-T model
		2,037[a]		
HD	1,750	1,980[a]	No surface	
		2,195[a]		

Basic building block: D-dried material (H/S ~ 0.8). These are experimental measurements. They are similar to 1.1 nm of tobermorite (H/C ~ 1.0) or matajennite (H/C ~ 0.8). Individual globules: Computed solid fraction is 82% (from packing factor) with interstitial spaces either empty or full. In this model they are full at 11% rh. These numbers can be compared to dehydrated crystalline equivalents. At 11% rh the computed value for density is the same as the measured value. However upon drying:

$$2{,}180\frac{FW(C_{1.7}SH_{0.8})}{FW(C_{1.7}SH_{1.2})} \sim 2100$$

or

$$2{,}440\frac{FW(C_{1.7}SH_{0.8})}{FW(C_{1.7}SH_{1.2})} \sim 2350$$

These numbers (2,100 kg/m^3 > 2,010 kg/m^3) or (2,350 kg/m^3 > 2,300 kg/m^3) imply that the crystalline equivalent loses less water on drying than does the amorphous C-S-H. LD: Packing 3.2 (2.8)-nm globules with 72% efficiency. HD: Packing 3.2 (2.8)-nm globules with 83% efficiency.

[a] Volume of pore and associated water depends on density of basic building block.

Table 5
Pore size

Technique	Radius (nm)	Comments	References
Nitrogen	1.3[a]	Experimental	
	4.0		
NMR	2.5	Experimental	[16,17]
	5.0		
SANS	2.5 (or less)	Possibly characteristic size of globule	[26]
Model	1.4 entrances	Packing 9.3-nm LD units	
	2.0 tetrahedral	Packing 9.3 nm	
	3.8 octahedral	Packing 9.3 nm	
	1.3 octahedral	Packing 3.2-nm globules	
	1.2 octahedral	Packing 2.8-nm globules	
	0.16 entrance	Packing 1.1-nm building blocks	
	0.24 tetrahedral	Packing 1.1-nm building blocks	
	0.45 octahedral	Packing 1.1-nm building blocks	

[a] Bimodal distribution.

cussed further in the section on coarse structure. If the radius is taken as a measure of the size of the "yardstick" used to see a given surface area, then the slopes can be used to compute fractal dimension [39]. The following formula relates mass (M) to density (ρ) as a function of r [see Eq. (3)]:

$$M \propto \rho r^3$$

$$\text{but } \rho(r) \propto r^{-.27}$$

$$M \propto \rho(r^{-.27})r^3$$

$$M \propto \rho r^{2.73} \tag{3}$$

The mass fractal is 2.73. This value, obtained from the model, compares favorably with values reported in the literature [37,38]. The volume surface fractal may be equivalent to the number of features seen at a given magnification or resolution. If so it scales with the size of the feature [40] according to Eq. (4):

$$S \propto r^{-(D-2)} \tag{4}$$

which gives $D = 2.74$.

Finally, a transition between surface and volume fractals has been observed at the length scale of about 20 nm (r = 10 nm), which is roughly the size of the LD C-S-H units in this model [38]. Interestingly, the volume or density fractal can be related to overall total porosity by Eq. (5) [40]:

$$\phi = \left(\frac{\ell_1}{\ell_2}\right)^{3-D_v} \tag{5}$$

where ℓ_1 and ℓ_2 are the upper and lower cutoff of the range where power law indicates fractal characteristics. Depending on the exact values chosen, ϕ is around 0.5. For example, if $\ell_1 = 1.2$ and $\ell_2 = 9.3$, then $\phi = 0.54$. LD C-S-H has a value of 0.5, computed directly.

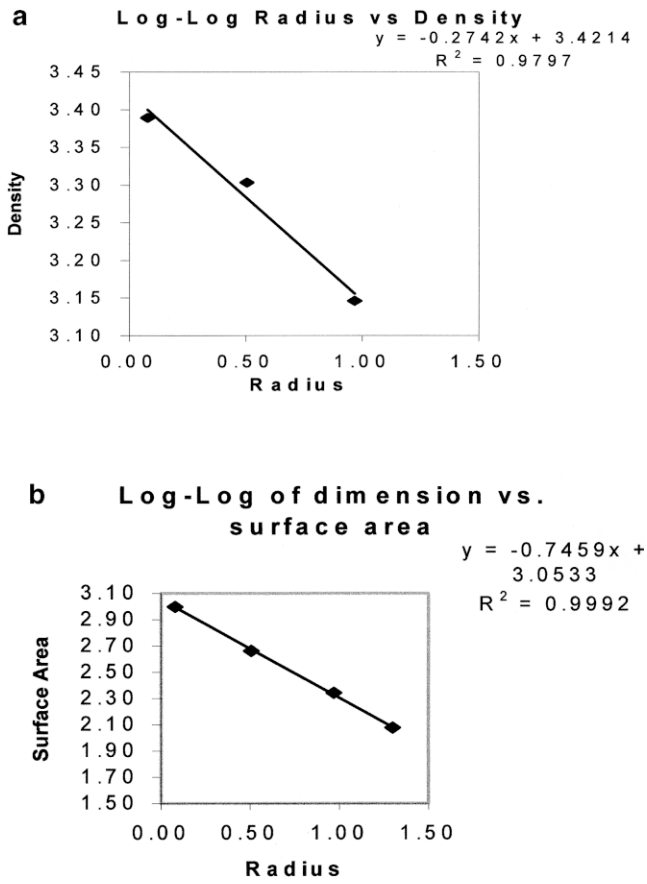

Fig. 5. Log-log plots: (a) density vs. radius; (b) surface area vs. radius. The best-fit line is included under the caption.

3.6. Comment on formation of structure

In colloidal systems it is common for particles to be made up of smaller units [41–43]. The structures reported here are fairly dense, and as argued by Scherer [44], they are probably precipitates that form in a partly reversible process involving restructuring of the initial arrangement of particles. This rearrangement densifies the structure. The relationship between structure at the level of the model and that on a coarser scale is discussed more fully later.

4. Comment on the structure <2 nm

Thus far, the model has been described as consisting of assemblages of uniform spheres of r = 1.2 nm. Obviously this is an oversimplification. The main reason is that the spheres have a volume and density as described. The volume is 7.24 nm^3. With this in mind, one possibility involves the formation of structure as shown in Fig. 6. As proposed by Taylor [45], the structure of C-S-H may be an intimate mixture of imperfect jennite (J) and tobermorite (T), with bridging silicate tetrahedra (represented as dotted triangles in Fig. 6) either missing or substituted by aluminum oxide. The representation of Fig. 6 is highly schematic and differ-

entiates between the structure of jennite and tobermorite simply by adding a row of calcium oxide with appropriate hydroxed ions as shown in Fig. 6b. This must also be accompanied by some geometric rearrangement that is not shown in Fig. 6. However, jennite and tobermorite are related. Thus, slightly different species react (Fig 6a) to form either J or T, and the conversion of T into J should be mechanistically possible in the presence of excess calcium and hydroxol groups or by some sequence such as that shown in Fig. 6d. This allows for the transformation of T into J, and it provides bridging tetrahedra for nearby J, which is in agreement with Taylor's hypothesis for the structure of C-S-H [45]. If tobermorite simply acquires bridging tetrahedra as C-S-H matures, it is difficult to see where they come from. Since both J and T can easily form a bimodal distribution of J and T, this would lead to bimodal C/S for which there is some evidence in relatively young cement [46].

This structure has a volume of 7.4 nm^3 based on atomic arguments, which is independent of the model described in this paper. In this structure, silicate chains five units long occur naturally. Also, this shape can pack much more effectively than spheres, which accounts for 82% packing factor. The problem with shapes other than a sphere is that the surface area per unit increases, in this case from 18 nm^2 per sphere to 24 nm^2 per unit. These numbers are far too precise, especially with bridging tetrahedra missing, and they are only meant to give rough ideas about the possibilities. If the units pack together in such a fashion that surfaces are removed (see Fig. 7b), and chain length increases to 11, for example, then the surface area will effectively be reduced back to that of a sphere. These are extremely small units and therefore have very large edge or surface effects. For example, the ratio in density between long-range order in the c direction and the units here with only two layers based on the dimensions in the c direction (Fig. 6), either including the average dimension over many layers or two layers, is $(2 \times 1.4)/2.54 = 1.1$. Interestingly, the two density ranges are $2{,}800/2{,}500 = 1.12$. Water may detect this basic unit more efficiently or completely than He does.

5. Drying C-S-H

This model has been developed from data obtained from saturated, nearly dried and D-dried samples. Only the X-ray method has been used to examine directly the effect of drying, and it is clear that drying reduces the measured surface area. Some sense of what happens during drying can be deduced.

In this model the structure of the globule with a radius of about 3.2 nm (2.8 nm) has formed by the end of the middle period. However, the structure of the LD C-S-H with $r = 9.3$ nm does not necessarily form until either (1) more time passes or (2) the sample is dried. Wet LD C-S-H could be much more open and drying or aging could cause significant restructuring, a process where units move toward the center of a cluster. It is tempting to suggest that aspects of both creep and shrinkage are related to this restructuring of the globules.

Since the results of Roper [47], the mechanisms of drying have been divided into four regions: (1) Drying to 90% rh produces relatively small shrinkage for the amount of water lost. Water is lost from large pores with associated small capillary stress. (2) Further drying down to 40% rh produces greater shrinkage for the amount of water lost, and this is attributed to smaller capillary pores and gel pores that are associated with larger stress. (3) A region between 40 and 20% rh exhibits relatively small shrinkage that is attributed to loss of adsorbed water and/or to the break up of menisci in pores less than about 3-nm radius. (4) Drying from 20 to 0% rh is accompanied by loss of interlayer water, causing irreversible collapse in the structure.

The model presented here is based on the idea that C-S-H is a colloid that forms a precipitate (as opposed to a gel that would fill all of the available space leaving no capillary porosity). This model offers some additional types of changes that occur on drying and mechanisms of drying shrinkage.

Using the Kelvin equation, it can be determined that upon drying to 85% rh, all pores with radius greater than about 10 nm are emptied. The capillary pores would be empty, but the pores in Figs. 3b, 3c, and 4 would remain full. The associated capillary stress is somewhere near a modest 10 MPa, and this causes only a small amount of shrinkage.

Drying to 40% rh causes this LD C-S-H (Fig. 3b) structure to collapse (possibly forming a structure like that in Fig. 3c), and large shrinkage occurs. This is a process that may be similar to the constant rate period [41] when a colloid gel first loses its water by surface evaporation and densification of solids. Large volume changes occur in colloids. This process for colloids typically does not involve evaporation from pores within the gel (i.e., the pores remain saturated), but for the structure proposed here, pores down to 1.5-nm radius empty. This means that at 40% rh, the N_2 accessible pores have emptied, and capillary stress works in combination with collapsing structure to cause shrinkage, although at lower rh the meniscus is certainly unstable. Since the separation between gel pore size and capillary pore size has never been defined exactly, and since a change in mechanisms of shrinkage appears to abruptly occur at about 40% rh [47], the idea that progressively smaller pores are being emptied, resulting in smoothly increasing stress and shrinkage, seems inadequate. However, the end of the constant rate period for colloids is abrupt and is called the "critical point," supporting the possibility that C-S-H behaves like a colloid in this respect. Furthermore, collapse according to constant rate period, with limited emptying of the pores within LD C-S-H, can be largely irreversible, as is observed on drying to 50% rh [20], while shrinkage resulting from capillary stress alone is reversible. Finally, according to the J-T model, more LD C-S-H forms at higher water/cement ratios, which would explain the direct relationship between irreversible shrinkage and pore volume.

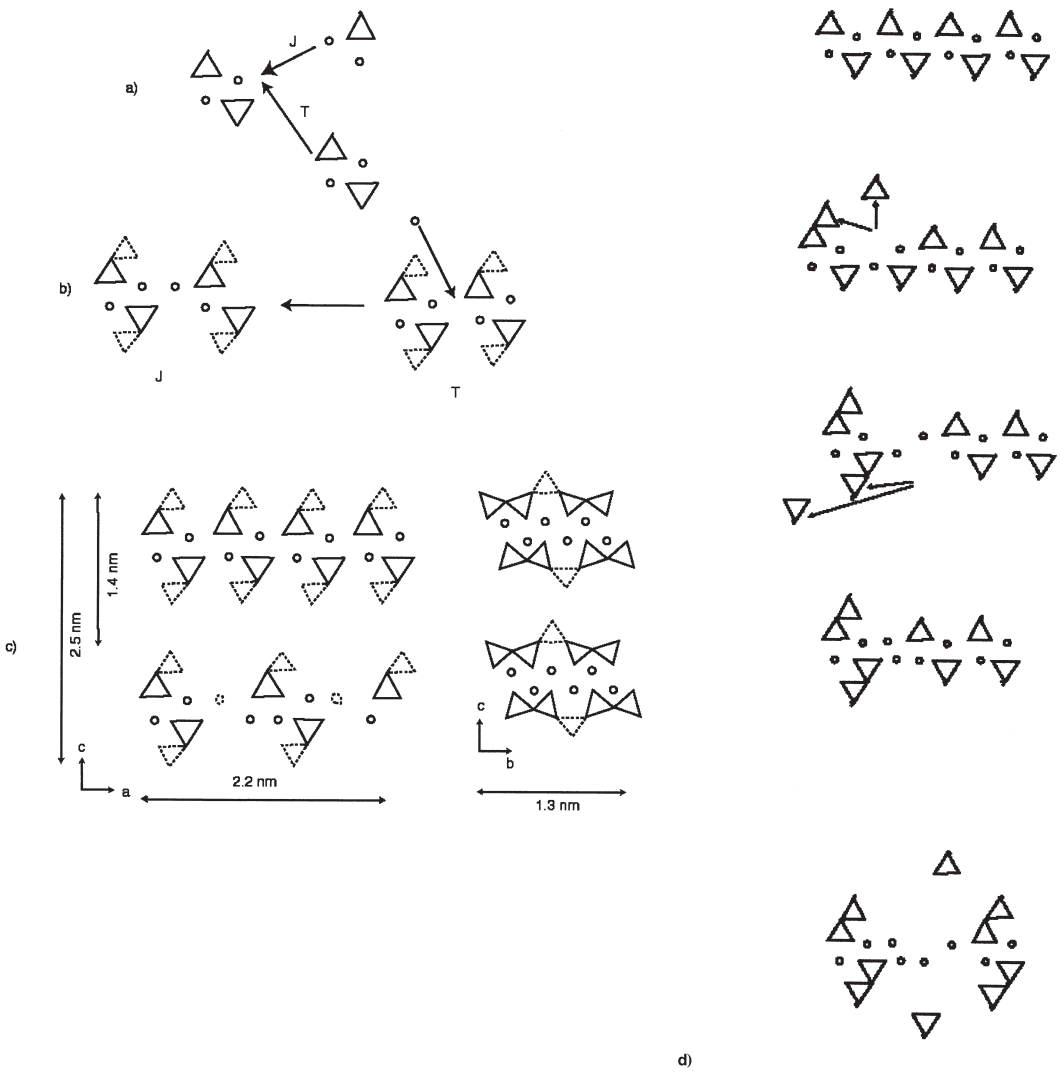

Fig. 6. Highly schematic sequence of assembling the basic unit. This representation is too ordered, but it is intended to show the relationship of jennite to tobermorite: (a) A small variation of the geometry of the dissolved reactants leads to a structure that is jennite-like (J) or tobermorite-like (T), typically without the bridging tetrahedra (dotted lines); (b) the simple layer; (c) approximate dimensions of the smallest unit; (d) transformation of the tobermorite-like to jennite-like units with average calcium silicon (c/s) = 1.7 as the bridging tetrahedra are placed by scavenging the structure for isolated tetrahedra. This schematic ignores OH^- that is required where the silicates are absent, and in Portland cement, substitution of bridging tetrahedra by aluminum and sulfate.

As mentioned previously, at about 40% rh an abrupt change in mechanism occurs, where the continued loss of water does not cause as much bulk shrinkage as it does from 90 to 40% rhs. The region between 40 and 20% rh may be analogous to the first falling rate period in colloids [42] when the menisci enter the gel pore system. Water is removed from the LD C-S-H and then from the HD C-S-H, but not from the globules. Because capillary stress no longer exists (in ceramics the first falling period can be accompanied by expansion), the amount of shrinkage would be reduced during this period. Experiments on very small unrestrained samples done in an environmental electron microscope have indeed shown expansion between 40 and 20% as shown in Fig. 7 [48]. This is direct evidence in support of this type of drying of a colloidal C-S-H.

An abrupt change again occurs at about 20% rh when multilayer desorption occurs. Its removal increases the surface energy of solids, which results in the classic Gibbs-Bangham shrinkage. This continues even below the 11% rh, when a monolayer has formed and the globules begin to empty in this model. As noted in Table 5, there is just enough room between the basic building blocks for a layer of water molecules on each surface within the globule. Large shrinkage occurs in both types of C-S-H.

Drying removes water first from the larger pores and then progressively from smaller and smaller pores. In this model, at 11% rh water is removed from all pores except from the globules with radius of 2.7 nm (2.4 nm), which, with a density of 2,180 kg/m^3 (2,450 kg/m^3), must have its porosity full. The problem is that without some sort of col-

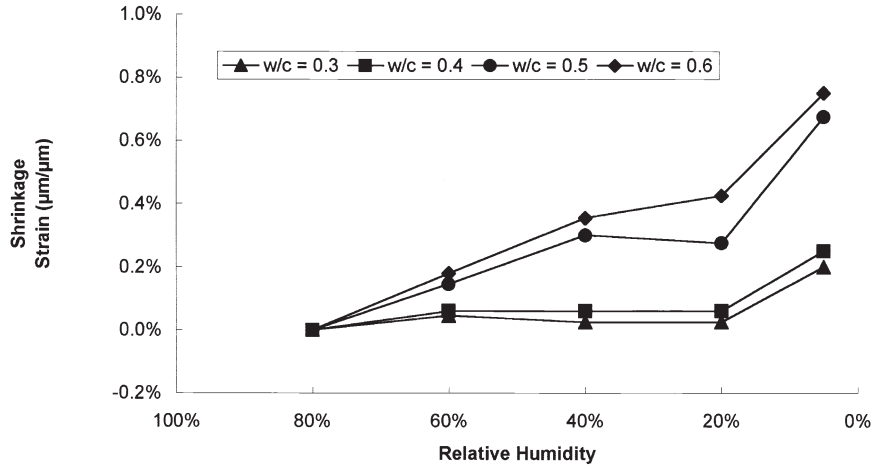

Fig. 7. Shrinkage water/cement ratio, age = 7 days (data taken from ref. [48]).

lapse of fine structure within the globules (without having lost any of its water), it is difficult to explain the loss of surface area as measured by X-rays at lower rhs. Somehow removing water from the spaces between the globules, but not from within the globules, changes the structure such that the basic units or the internal structure of globules cannot be resolved by X-rays. This problem must have something to do with the high stress of removing water from the 1.3 nm and smaller (radius) pores between the globules, and this would be similar to the stresses that cause collapse during the constant rate period except that now this stress is applied to the smaller globules. These stresses may align the fragments of sheets that make up the basic unit, as is qualitatively suggested in Fig. 8. Thus, although the volume of the basic unit does not change, the alignment and shape does. It may be that this alignment, or changes in alignment, is related to other properties such as creep. Indeed, surface areas [49,50] have been shown to change as a result of applied load over a period of time. These spaces between the basic units are perhaps akin to the interlayer space, as described by Ramachandran et al. [51].

As shown in the footnote of Table 4 (based on HFW Taylor personal communication), it appears that the C-S-H in cement loses more water upon drying from 11% rh to D-dry than does its crystalline equivalent. This makes sense because the small units in Figs. 6 and 8 have more surfaces in the a and b directions than their crystalline equivalent, and therefore more water is adsorbed on these surfaces and in the related pore space. Furthermore the pores within the globule may contain more water than would strictly be a monolayer, which is what statistically occurs at 11% rh. Maybe these pores are full at 20% rh and then empty, and associated rearrangements cause the final high shrinkage.

It is possible that at 11% rh, the water in the pores, which are extremely small, has a density higher than 1,000 kg/m^3. This may help explain the higher measured value for density, in which case the volume of pores in the globule would be less than 19%. If this is so, contrast between solid and water is small and X-rays do not scatter, thus lowering the measured SSA.

If C-S-H is very carefully dried by lengthy solvent exchange followed by fast D-drying, LD C-S-H remains open enough to allow N_2 to penetrate and measure the 3.2 nm (2.8 nm) globules. This means that N_2 "sees" a surface area equivalent to that of the globules measured by SANS (see Table 2). However, under normal direct D-drying, the C-S-H collapses, and only the LD structure is measured. This reasoning is the basis for the J-T model. Upon more severe drying (such as oven drying) the SSA is reduced, suggesting that the LD structure also has collapsed, which results in a reduced gel pore volume compared to that of carefully dried samples. Values of SSA for oven-dried samples using N_2 do not vary strongly with water/cement ratio and are roughly equivalent to values obtained by using isopropanol sorption, suggesting that the interstitial spaces have become smaller. These SSAs could be associated with features having r = 20 nm or more, and are within the size range of the resolution of scanning electron microscopy.

The model described here can account for the hysteresis in length change, modulus, and weight gain of paste with change in moisture content in essentially the way described by Ramachandran et al. [51]. However, instead of water entering only the interlayer space to cause changes in the bulk, it moves in and out of the pores at each scale in this model. When water is removed, the structure at that scale collapses as just described for the finest scale, perhaps the new equivalent of the interlayer space. When the structure collapses (i.e., if the globules become entwined as water is removed and as rh is lowered at intermediate rh) the addition of water does not cause equivalent expansion at the same rh. This may be because the pores at any one scale always have entrances that are smaller than the pore, no matter which scale is considered. As the result of multiple-sized ink bottle pores, the observed hysteresis clearly would result.

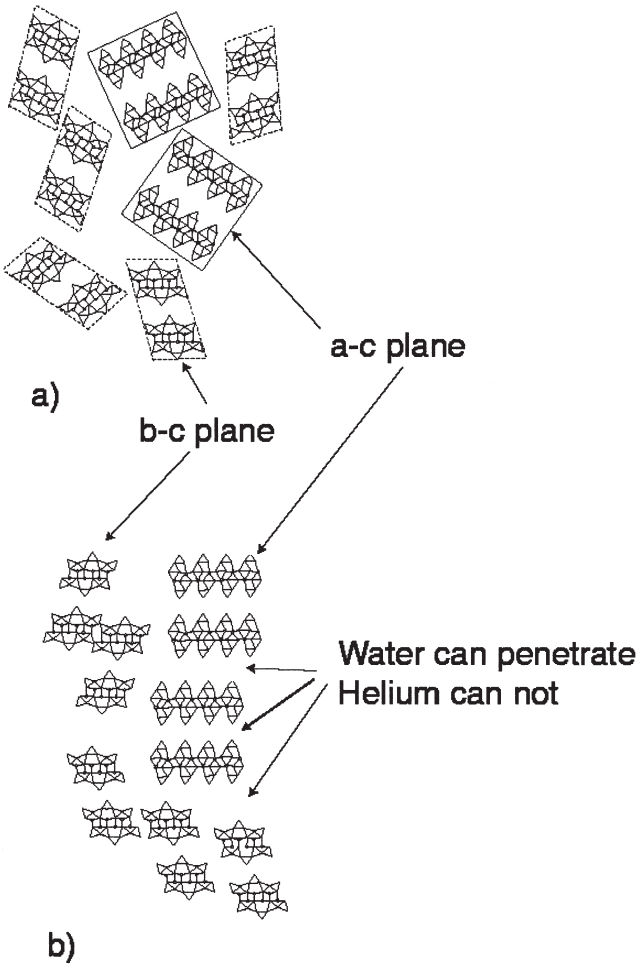

Fig. 8. Packing of the basic units (a) wet and (b) dry. The orientations of the basic units are arbitrarily two orthogonal views and are not meant to indicate that the real structure is this organized; it is certainly much more random, and this picture is simply a first approximation of possible packing.

6. Coarser structure

Only broad comments can be made about the relationship between the structure described by this model and microstructure as seen in an electron microscope. The following are possibilities.

The HD C-S-H is similar to inner product, but the boundary between it and other products is not the surface of the original unreacted cement but rather a surface of the unreacted grains at the beginning of the late period. This may also be the C-S-H portion of phenograins (phenograms include unreacted cement and other dense material). In other words, it is fairly dense and apparently structureless. Although LD C-S-H forms almost exclusively during the early period and HD C-S-H is more abundant during the late stage, some LD C-S-H continues to form (Ca must be expelled from unreacted grains) during the late stages.

Many scanning electron microscopy and transmission electron microscopy (TEM) investigations have shown that the outer product C-S-H is composed of more open and friable morphologies, and it is not immediately obvious how these could be made up of globules such as those proposed in the present model. However, as described by Brinker and Scherer [41], colloid science is full of examples of particles made up by the aggregation of smaller particles. This aggregation forms precipitates. Brinker and Scherer [41] point out that this often results from an asymmetric electric double layer surrounding the basic unit. This can result in sheets [52] and other forms and structures, which could crumple and roll up to form other morphologies such as needles [53]. A number of examples are provided in chapter 4 of Matijevic's work [44]. According to this model, they are all precipitated LD C-S-H. Also, the precipitation process could lead to regions of local crystallization. Even after precipitation, the individual particles could rearrange.

As shown in Fig. 5b, a low surface area of 120 m^2/g, as measured by larger molecules, might be associated with features about 40 nm across (0.04 μm). Diamond's Type III has 0.1 μm [54] characteristic dimensions, which may represent the finest structure of C-S-H. If all of the morphologies observed in dried paste are made of packed particles of the order of 40 nm across, then pores would have entrances of between 6 and 16 nm across depending on how tightly packed the particles are, and internal diameters of between 10 and 16 to 28 nm, depending on if they are tetrahedral, octahedral, or cubic. NMR [16,17] has measured diameters of between 20 to 25 nm, labeled capillary pores, but this may be the larger internal gel pores according to this model.

7. Influence of reaction conditions

This model has been illustrated for water/cement ratio = 0.4 where, in mature samples, about 50% of the C-S-H is LD and the rest is HD. The initial amount of water in the water/cement ratio influences the ratio of LD to HD types [27]. This may be because the precipitation (coagulation) process does not start until the fraction of solids reaches a certain concentration, and the more water that is present, the more the solids that are necessary to reach the critical volume fraction necessary for precipitation. Different drying conditions alter the structure in different ways, and different parts of the structure are seen by different techniques. According to the J-T model, variables such as water/cement ratio and the presence of chemical and mineral admixtures alter the amount of LD and HD types. This model can be extrapolated to other formulations, therefore, by deducing the amount of LD C-S-H from the J-T model or by measuring the nitrogen surface area of samples dried carefully [27].

With the passage of time and/or with increased temperature, the length of the silicate chain is known to increase. This may be accomplished by silicate tetrahedra bridging particles and, in effect, making them larger. This could only be accomplished in a collapsed version of LD C-S-H as described in the sections on drying. Thus both age and temperature precollapse (preshrink) the LD C-S-H. Perhaps this is part of the explanation of why both age and temperature re-

duce shrinkage; it has already shrunk. Certainly the irreversible part would be reduced. Indeed, with increased temperature (or the passage of time, not shown) the shrinkage in the 90 to 40% rh is greatly reduced in very small samples as shown in Fig. 7 [48]. This could be interpreted as evidence that at higher temperatures (or with the passage of time), the C-S-H collapses by itself. In effect it becomes preshrunk.

This model suggests that all of the morphologies that form the microstructure of C-S-H in pastes are the result of either precipitating basic units that form LD C-S-H or densely packed units that form HD C-S-H. There is no sense of one- or two- or three-dimensional growth, a necessity of hollow needles or solid needles that form by chemical growth. The morphologies are the result of precipitation of basic units within the capillary pores, and probably the result of different kinetics. Thus many arguments in the literature become irrelevant. The influence of temperature may be strong. High temperatures decrease SSA, but they increase the chain length. The basic units may get larger at higher temperature and/or they may bond together with bridging tetrahedra. Also it is almost certain that additives such as slag will influence strongly the ratio of LD to HD C-S-H.

8. Comment on density

The results of this model do not determine which density of the basic unit is correct, although there might be a slight bias toward the higher density. This is consistent with a measured (not calculated) density for 11% rh C-S-H as well as being roughly the size of the globules as measured by SANS [25,26] and recent interpretation of SANS contrast data. If this is true, than He and methanol are not entering the finest pores (Table 3), but they do see the globules, which is in agreement with the model density. This density is higher than that of tobermorite, presumably because of the missing silicate tetrahedra.

9. Overview of the model and summary

The model described here has as its justification a consistency with various measurements. It quantitatively relates surface area, density, and size of units with particular units measured by a particular technique. Like the successful Feldman-Sereda model, it is an attempt to find a hidden structure that is consistent with measured quantities. Parts of the model have not yet been optimized because of insufficient data, and therefore some of the numbers may well be altered or refined in the future. The purpose of this model is to stimulate discussion and especially to indicate the direction of future experimental work.

Perhaps the most important feature of the model is the presumption of two types of C-S-H. The surface area of the HD type is not detected by several techniques, and this is the root cause of so many different values in the literature. Both types are made of basic building blocks that form into globules that have two possible packing arrangements.

The model as presented here is for C-S-H in an average cement paste, and it is almost certain that some parameters, such as the amount of the LD product, will vary with the methods of processing, such as variations in the initial water/cement ratio, temperature of reaction, and presence of admixtures. The J-T model so far accounts for only the influence of water/cement ratio, but it is hoped that it will serve as a basis for a complete quantitative model that accounts for variation in processing and composition.

The model is a quantitative description of the structure of calcium silicate hydrate between 1 and 100 nm. The important features include the following: (1) A specific technique for measuring the SSA resolves a specific fineness in the structure. This is the main reason why different techniques measure different SSAs. (2) Nitrogen SSA varies for two main reasons: drying procedure and reaction conditions such as water/cement ratio. The latter reason is related to the quantity of LD and HD C-S-H, and thus nitrogen SSA is a measure of this part of the microstructure. (3) Water fills the pore space starting with the finest pores at the lowest rh, and this is the basis for computing the densities expected at different rhs. (4) The surface area as measured by SANS is associated with scattering from globules with a density and composition equal to that of C-S-H equilibrated with 11% RH, and the globules are surrounded by water. (5) The structure is fractal. (6) Even though approximate, the measured size of gel pores is compatible with the size of pores in the model structure. (7) Remarks 1 through 6 above are quantitatively self-consistent.

Thus, the model is basically units that pack to form globules, which in turn pack together to form LD and HD C-S-H structures. These units pack together to form the microstructure of C-S-H. The model defines the size, density, and packing efficiency of each of these structures so that many experimental observations are rationalized. The principal advantage over other models is that at each scale, this model is quantitative, which may be related to properties.

Acknowledgments

I gratefully acknowledge the financial support provided by the U.S. Department of Energy (Award DE-FG02-91ER45460), and the insight and ideas provided by G. Frondsdorff, H.F.W. Taylor, J.F. Young, and J.J. Thomas.

References

[1] H.F.W. Taylor, Cement Chemistry, 2d ed., Thomas Telford Publishing, London, England, 1997.
[2] X. Cong, J.R. Kirkpatrick, O MAS NMR investigation of the structure of calcium silicate hydrate gel, J Am Ceram Soc 79 (6) (1996) 1585–1592.
[3] A.R. Brough, C.M. Dobson, I.G. Richardson, G.W. Groves, Applica-

tion of selective ^{29}Si isotopic enrichment to studies of the structure of calcium silicate hydrate (C-S-H) gels, J Am Ceram Soc 77 (2) (1994) 593–596.
[4] X. Cong, R.J. Kirkpatrick, ^{29}Si and ^{17}O NMR investigation of the structure of some crystalline calcium silicate hydrates, Advn Cem Bas Mat 3 (1996) 133–143.
[5] H.F.W. Taylor, Proposed structure for calcium silicate hydrate gel, J Am Ceram Soc 69 (6) (1986) 464–467.
[6] R.F. Feldman, P. Sereda, A new model for hydrated Portland cement and its practical implications, Eng J Can 53 (8–9) (1970) 53–59.
[7] F.H. Wittman, The structure of hardened cement paste—A basis for a better understanding of the materials properties, in: Hydraulic Cement Pastes: Their Structure and Properties. Cement and Concrete Association, Slough, United Kingdom, 1976, pp. 96–117.
[8] S. Brunauer, Tobermorite gel—The heart of concrete, American Scientist 50 (1962) 210–229.
[9] M. Daimon, S.A. Abo-El-Enein, G. Hosaka, S. Goto, R. Kondo, Pore structure of calcium silicate hydrate in hydrated tricalcium silicate, J Am Ceram Soc 60 (1977) 110–114.
[10] J.J. Thomas, H.M. Jennings, A.J. Allen, The surface area of hardened cement paste as measured by various techniques, Concrete Science and Engineering 1 (1999) 45–64.
[11] J.J. Thomas, H.M. Jennings, Effects of D_2O and mixing on the early hydration kinetics of tricalcium silicate, Chem Mater 11 (1999) 1907–1914.
[12] S. Fitzgerald, D. Neumann, J. Rush, D. Bentz, R.A. Livingston, An in-situ quasi elastic neutron scattering study of the hydration of tricalcium silicate, Chemistry of Materials 10 (1998) 397–402.
[13] H.M. Jennings, B.J. Dalgleish, P.L. Pratt, Morphological development of hydrating tricalcium silicate as examined by electron microscope techniques, J Am Ceram Soc 64 (1981) 567–572.
[14] I. Jawed, J. Skalny, J.F. Young, Hydration of Portland cement, in: P. Barnes (Ed.), Structure and Performance of Cements, Applied Science Publisher, Essex, United Kingdom, 1983, pp. 237–318.
[15] D.N. Winslow, J.M. Bukowski, J.F. Young, The early evolution of the surface of hydrating cement, Cem Con Res 24 (6) (1994) 1025–1032.
[16] J.Y. Jehng, Microstructure of wet cement pastes, Ph.D. thesis, Northwestern University, Evanston, IL, 1995.
[17] W.P. Halperin, J.Y. Jehng, Y.Q. Song, Application of spin-spin relaxation to measurement of surface area and pore size distributions in a hydrating cement paste, Magn Reson Imaging 12 (12) (1994) 169–173.
[18] J.J. Thomas, H.M. Jennings, A.J. Allen, The surface area of cement paste as measured by neutron scattering—Evidence for two C-S-H morphologies, Cem Concr Res 28 (6) (1998) 897–905.
[19] C.M. Hunt, Nitrogen sorption measurements and surface areas of hardened cement paste, in: Symposium on Structure of Portland Cement Paste and Concrete, Highway Research Board Special Report 90, Washington, D.C., 1966, pp. 112–122.
[20] M.C. Garci, Quantifying microstructural variations in cement pastes: Implications on drying shrinkage, Ph.D. thesis, Northwestern University, Evanston, IL, 1999.
[21] D.L. Kantro, S. Brunauer, C.H. Weise, Development of surface in the hydration of calcium silicates, J Phys Chem 66 (1962) 1804–1809.
[22] D.N. Winslow, S. Diamond, Specific surface of hardened cement paste as determined by small-angle X-ray scattering, J Am Ceram Soc 57 (5) (1974) 193–97.
[23] J.J. Volkl, R.E. Beddoe, M.J. Setzer, The specific surface of hardened cement paste by small-angle X-ray scattering—Effect of moisture content and chlorides, Cem Concr Res 17 (1987) 81–87.
[24] R.E. Beddoe, K. Lang, Effect of moisture on fractal dimension and specific surface of hardened cement paste by small-angle x-ray scattering, Cem Concr Res 24 (4) (1994) 605–612.
[25] J.J. Thomas, H.M. Jennings, A.J. Allen, Determination of the neutron scattering contrast of hydrated Portland cement paste using H_2O/D_2O exchange, Adv Cem Bas Mat 7 (3) (1998) 119–122.
[26] A.J. Allen, R.C. Oberthur, D. Pearson, P. Schofield, C.R. Wilding, Development of the fine porosity and gel structure of hydrating cement systems, Phil Mag B 56 (3) (1987) 263–268.
[27] P.D. Tennis, H.M. Jennings, A model for two types of C-S-H in the microstructure of cement paste, Cem Concr Res (in press).
[28] G.G. Litvan, Variability of the nitrogen surface area of hydrated cement paste, Cem Concr Res 6 (1976) 139–144.
[29] L.J. Parrott, Effect of drying history upon the exchange of pore water with methanol and upon subsequent methanol sorption behavior in hydrated alite paste, Cem Concr Res 11 (1981) 651–658.
[30] R. Sh Mikhail, S.A. Selim, Adsorption of organic vapors in relation to pore structure of hardened Portland cement paste, in Symposium on Structure of Portland Cement Paste and Concrete, Highway Research Board Special Report 90, Washington, D.C., 1966, pp. 123–134.
[31] R.F. Feldman, Helium flow and density measurement of the hydrated tricalcium silicate—Water system, Cem Concr Res 2 (1972) 123–136.
[32] T.C. Powers, T.L. Brownyard, Studies of the Physical Properties of Hardened Portland Cement Paste (Bull. 22), Portland Cement Association, Chicago, IL (1948); reprinted from J Amer Concr Inst Proc 43 (1947) 469–504.
[33] S. Brunauer, S.A. Greenberg, The hydration of tricalcium silicate and β-dicalcium silicate at room temperature, in: 4th ISCC, Vol. 1, National Bureau of Standards, Washington, D.C., 1962, pp. 135–165.
[34] M. Relis, J. Soroka, Limiting values for density, expansion and intrinsic shrinkage in hydrated Portland cement, Cem Concr Res 10 (4) (1980) 499–508.
[35] W. Hansen, (1987) quoted by J.F. Young and W. Hansen, in: J.F. Young, W. Hansen, Volume relationships for C-S-H formation based on hydration stoichiometries, Mater Res Soc Symp Proc 85 (1987) 313–322.
[36] H.M. Jennings, P.D. Tennis, Model for the developing microstructure in Portland cement pastes, J Am Ceram Soc 77 (12) (1994) 3161–3172, and correction 78 (9) (1995) 2575.
[37] A.J. Allen, R.A. Livingston, Small-angle scattering study of concrete microstructure as a function of silica fume, fly ash, or other pozzolanic additions, in: V.M. Malhotra (Ed), Proc. 5th CANMET/ACI Int. Cont. on Fly Ash, Silica Fume, Slag and Natural Pozzolans in Concrete, American Concrete Institute, Detroit, MI, 1995, pp. 1179–1200.
[38] D. Winslow, J. Bubowski, J.F. Young, The fractal arrangement of hydrated cement paste, Cem Concr Res 25 (1995) 147–156.
[39] J. Feder, Fractals, Plenum Press, New York, 1988.
[40] A.J. Katz, A.H. Thompson, Fractal sandstone pores: Implications for conductivity and pore formation, Phys Rev Let 54 (1985) 1325–1328.
[41] C.J. Brinker, G.W. Scherer, Sol-Gel Science, Academic Press, San Diego, 1990.
[42] E. Matijevic, Monodispersed colloids: Art and science, Langmuir 2 (1985) 12–20.
[43] E. Matijevic, Monodispersed metal (hydrous) oxides—A fascinating field of colloid science, Acc Chem Res 14 (1981) 22–29.
[44] G.W. Scherer, Structure and properties of gels, Cem Concr Res 29 (1999) 1149–1157.
[45] H.F. Taylor, Proposed structure for calcium silicate hydrate gel, J Am Ceram Soc 69 (6) (1986) 464–467.
[46] I.G. Richardson, G.W. Groves, Microstructure and microanalysis of hardened ordinary Portland cement pastes, J Mat Sci 28 (1993) 265–277.
[47] H. Roper, Dimensional change and water sorption studies of cement paste, in: Symposium on Structure of Portland Cement Paste and Concrete, Highway Research Board Special Report 90, Washington, D.C., 1966, pp. 74–83.
[48] T.B. Bergstrom, An environmental scanning electron microscope investigation of drying cement paste: Drying shrinkage, image analysis, and modeling, Ph.D. thesis, Northwestern University, Evanston, IL, 1993.
[49] A. Bentur, N.B. Milestone, J.F. Young, Creep and drying shrinkage of calcium silicate pastes: II. Induced microstructural and chemical changes, Cem Concr Res 8 (1978) 721–732.

[50] C.M. Neubauer, On the chemistry, micostructure, and deformation of cement pastes: Towards a new strategy for controlling drying shrinkage, Ph.D. thesis, Northwestern University, Evanston, IL, 1997.
[51] V.S. Ramachandran, R.F. Feldman, J.J. Beaudoin, Concrete Science: Treatise on Current Research, Heyden & Son, London, 1981.
[52] R.K. Iler, The Chemistry of Silica, John Wiley & Sons, New York, 1979.
[53] H.M. Jennings, P.L. Pratt, The use of high voltage electron microscope and gas reaction cell for the microstructural investigation of wet Portland cement, J Mat Sci 15 (1980) 250–253.
[54] S. Diamond, Cement paste microstructures: An overview at several levels, in: Hydraulic Cement Pastes: Their Structure and Properties, Proceedings of Conference at the University of Sheffield, Cement and Concrete Association, 1976, pp. 2–30.